On the deployment of V2X roadside units for traffic prediction

Lejun Jiang[a,b,*], Tamás G. Molnár[a,c], Gábor Orosz[a,d]

[a] *Department of Mechanical Engineering, University of Michigan, Ann Arbor, MI 48109, USA*
[b] *School of Engineering and Applied Science, University of Pennsylvania, Philadelphia, PA 19104, USA*
[c] *Department of Mechanical and Civil Engineering, California Institute of Technology, Pasadena, CA 91125, USA*
[d] *Department of Civil and Environmental Engineering, University of Michigan, Ann Arbor, MI 48109, USA*

Abstract

In this paper, we evaluate the ability of connected roadside infrastructure to provide traffic predictions on highways based on the motion of connected vehicles. In particular, we establish metrics to quantify the amount of traffic prediction that is available from roadside units via vehicle-to-infrastructure (V2I) communication. We utilize analytical and numerical tools to evaluate these metrics as a function of (i) the location of the roadside units along the road, (ii) the communication range of the roadside units, and (iii) the penetration rate of connected vehicles on the road. We show that considerable amount of traffic predictions can be achieved even with sparsely distributed roadside units as distant as two thousand meters and with connected vehicle penetration rate as low as 2%. Based on the proposed metrics, we develop strategies for deploying roadside units along highways so that traffic prediction efficiency is maximized. Ultimately, the results of this paper may serve as a guideline for evaluation and deployment of connected roadside infrastructure.

Keywords: vehicle-to-infrastructure connectivity, roadside unit, connected vehicle, traffic prediction

1. Introduction

Wireless vehicle-to-everything (V2X) communication technology has the potential to significantly improve the efficiency of road transportation systems. This technology includes vehicle-to-vehicle (V2V) and vehicle-to-infrastructure (V2I) communication, allowing vehicles and the infrastructure to share information within a few hundred meter radius. This opens the path for many applications targeting safety and efficiency [1].

In this work, we focus on applications that involve V2I communication [2] between connected vehicles (CVs) and roadside units (RSUs). The benefits of V2I connectivity has attracted considerable research interest in the past years [3]. Establishing and maintaining a connected roadside infrastructure, however, is associated with considerable costs, which makes the RSUs precious resources that should be allocated carefully. Therefore, significant effort has been devoted in the literature to study the optimal deployment of RSUs so that costs are minimized while selected performance measures are maximized.

Most of the literature frames the RSU deployment problem in the context of urban environments with dense RSU arrangements. These works either aim to maximize coverage, defined as the number of vehicles connected to the RSUs, subject to given cost constraints, or aim to minimize the data delivery delay in communication. For example, [4] introduces a cost efficient RSU deployment scheme to guarantee that CVs can reach RSUs within certain driving time. [5] uses binary integer programming to minimize the cost of full coverage. [6] proposes a density-based RSU deployment policy where RSU locations are designed based on expected traffic density to facilitate emergency services with minimal accident notification time. [7] frames the RSU deployment problem so that data delivery delays are improved. [8] proposes a genetic algorithm for RSU allocation to reduce warning notification times and improve vehicular communication capabilities, while [9] uses a genetic algorithm to maximize the coverage of RSU deployment.

*Corresponding author
Email addresses: lejunj@umich.edu (Lejun Jiang), tmolnar@caltech.edu (Tamás G. Molnár), orosz@umich.edu (Gábor Orosz)

Table 1: Nomenclature.

Symbol	Name	Symbol	Name
w	wave speed	T	duration of coverage zone
d_{st}	standstill distance	λ	peneration rate of connected vehicles
τ	time gap	C	coverage rate
N	number of follower vehicles	T_{tot}	total time covered
x_{RSU}	location of RSU	D	distance of two subsequent RSUs
R	communication range of RSU	D_{c}	critical distance for RSU placement

[10] solves the delay-bounded and cost-limited RSU deployment problem via a binary differential evolution scheme to maximize coverage. [11] proposes a spatiotemporal RSU deployment framework to optimize coverage ratio, deployment cost, network latency and overhead. [12] pursues the idea of deploying mobile RSUs to maximize coverage in a cost effective manner using integer linear programming. [13] aims to achieve optimum link flow determination via RSU deployment based on nonlinear binary integer programming.

Most of the above works address the trade-off between the overall communication quality and the total cost of the connected roadside infrastructure in urban environments. Providing *traffic predictions* by the roadside infrastructure, however, has not yet been considered in the literature as an aspect for RSU deployment. Moreover, RSU deployment on highways gets less attention in the literature, due to the simple geometry of highways compared to urban road networks. Yet, designing optimal placement for RSUs along highways is also relevant, as they may provide valuable traffic predictions for the vehicles passing by. In particular, forecasts about upcoming traffic congestions may be useful for vehicles to optimize their speed and lane selection. This ultimately leads to better overall efficiency and throughput of the traffic flow.

In this work, we intend to address these gaps. We introduce a new perspective to the RSU deployment problem. We view coverage not from the perspective of being able to communicate to at least one RSU at certain locations, but from the perspective of traffic predictions on highways. We say that a location is covered if it is possible to predict the future traffic at this location based on the information that the RSUs collect from CVs, and we seek to maximize coverage in this context.

There already exists a number of works on highway traffic state estimation and prediction that are potentially suitable for our purpose. [14] describes statistics-based and machine learning-based traffic prediction methods in the intelligent transportation systems framework. [15] surveys model-driven, data-driven, and streaming-data-driven approaches for traffic state estimation. [16] presents a strategy for real-time density estimation for traffic networks. [17] presents a technique to incorporate mobile probe measurements into highway traffic flow models. [18] introduces a short-term traffic flow prediction algorithm based on an adaptive multi-kernel support vector machine with spatial–temporal correlation. These prediction methods generate location-based predictions that are commonly used in the field, including the algorithms in routing apps (such as Waze, Google Maps, Here Maps or TomTom).

In this paper, we focus on traffic predictions that instead are based on recording the trajectories of CVs and processing them via the connected roadside infrastructure [19, 20, 21]. This idea can be found in [19, 22] in the context of V2V connectivity, whereas now we focus on predictions via V2I communication. The advantage of such V2I connectivity-based traffic forecasts is that they can be made real time and they can be tailored to needs of individual vehicles. Thus, they can supplement existing data-intense, location-based, higher-latency traffic forecasts provided by routing apps. This also makes our traffic prediction-based coverage less demanding in the sense that predicting future traffic does not require the knowledge of traffic conditions everywhere along the road, that is, full coverage w.r.t. predictions does not require full coverage w.r.t. communication. Partial observation of the traffic flow already allows reconstructing, estimating and predicting traffic [23, 24, 25, 26]. We investigate how V2I communication may facilitate traffic prediction even for sparse penetration of CVs and sparsely distributed roadside infrastructure. We will show that using our method even a single CV communicating with a single RSU can allow one to provide traffic forecasts. In order to maximize the amount and accuracy of available traffic predictions, the number and placement of the available RSUs are crucial, especially because the RSUs have limited communication range. We show how the

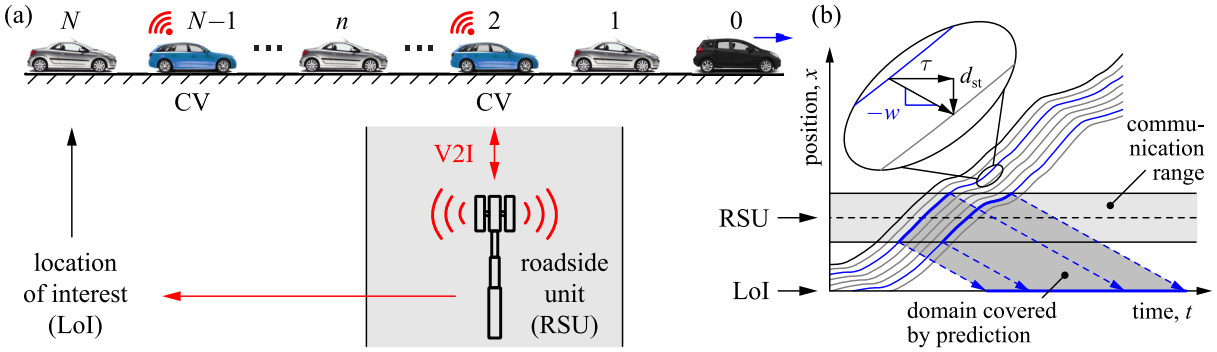

Figure 1: (a) Traffic flow consisting of non-connected (gray) and connected vehicles (blue), where a roadside unit provides traffic prediction for a location of interest. (b) Illustration of the vehicle trajectories, the RSU's communication range, and the region where traffic prediction is possible.

placement and communication range of RSUs as well as the penetration rate of CVs affect the availability of traffic predictions. The presented results can be translated into deployment strategies for RSUs that can collect traffic data and provide real-time forecasts.

The rest of the paper is organized as follows. Table 1 contains the nomenclature of the paper. Section 2 outlines our concept about how traffic prediction can be provided in real time for individual vehicles by connected roadside infrastructure. To conduct a quantitative case study, Section 3 introduces a data set where traffic is simulated based on a single measured CV trajectory. Section 4 introduces metrics to quantify the amount of available traffic predictions, and shows how the RSU location, the communication range and the penetration of CVs affect these metrics for the case of a single RSU. Section 5 extends the results for multiple RSUs and discusses deployment strategies to maximize the available traffic predictions. Section 6 summarizes the results and concludes the paper.

2. Traffic Prediction via Connected Roadside Infrastructure

In this section, we lay down the basic principles for utilizing roadside units (RSUs) for traffic monitoring and prediction via vehicle-to-infrastructure (V2I) communication. The method proposed here fundamentally differs from traditional traffic monitoring that collects information about the flux (flow rate) and the speed at a fixed location using cameras and loop detectors [27, 28, 29]. Instead, RSUs monitor the motion of vehicles that are equipped with V2X communication units, referred to as connected vehicles (CVs), while these are traveling in the RSUs' communication range. This provides high resolution velocity data along a few hundred meters long section of the highway that is not possible to obtain using cameras and loop detectors. We demonstrate below that even for low penetration of CVs this setup allows us to provide traffic forecasts for large spatial and temporal domains.

Consider the scenario in Fig. 1(a) where a string of vehicles is traveling on a highway, consisting of non-connected vehicles and connected vehicles, as indicated by gray and blue colors, respectively. Let us number the vehicles with an index n increasing upstream starting from a lead vehicle $n = 0$ highlighted by black. We seek to provide predictions about the future state of traffic at a certain location of interest (LoI) along the highway based on the motion of CVs ahead. For example, if we know that a CV is slowing down due to a traffic congestion downstream the LoI, then we may predict when and how much the traffic speed will decrease at the LoI due to the propagation of the congestion. Note that although we focus on prediction provided for a specific LoI, this location is arbitrary, and there could be a range of locations, or a section of road that receives the prediction.

In order to achieve this goal, we propose to utilize roadside units as depicted in Fig. 1(a) whose communication range is highlighted by light gray shading. Such infrastructure is able to collect information about the motion of CVs and compute traffic forecasts from the available trajectories. To this end, consider the trajectories in Fig. 1(b) where the positions of the vehicles are depicted as a function of time. The trajectories of CVs are highlighted as blue with thick sections within the light gray shaded communication range of the RSU. These thick pieces of trajectories indicate the information that is available to the RSU about the motion of CVs. The motion of CVs affects the motion of other vehicles behind them over specific time intervals such that the vehicles traveling farther behind are affected later in time. This is illustrated by the blue arrows and gray shading. The information available to the RSUs (thick

blue trajectories) enables traffic prediction in these specific domains of space and time (dark gray region). If one intends to predict traffic at a location of interest (here considered to be the horizontal axis $x = 0$), then predictions can be made during the time intervals where the dark gray shaded domain intersects the LoI; see thick blue section.

Notice that there are time domains where multiple CV trajectories can be used for predictions despite the fact that a low CV penetration rate is illustrated in the figure. This is due to the fact that the RSU has a finite communication range. Our goal is to relate the RSU's communication range and the penetration rate of CVs to the amount of available traffic predictions at the LoI. In order to predict the motion of non-connected vehicles, we use continuum traffic models. In our numerical case studies, CVs are mixed into the flow of non-connected vehicles in a random fashion. Finally, we also consider scenarios when traffic predictions are generated by multiple RSUs at the same time.

3. Lagrangian Traffic Flow Simulation

As a basis for this study, we simulate highway traffic while utilizing experimental data for the lead vehicle. The simulated traffic flow will be used to study how traffic predictions can be facilitated by RSUs. While there exist a large number of models with different levels of sophistication [30] to describe traffic flow, here we consider one of the simplest continuum models called Lighthill-Whitham-Richards (LWR) model [31, 32]. This model is typically written in the Eulerian framework [33, 34, 35] describing the traffic states at a fixed location along the highway. However, in our problem the RSU is collecting trajectory data from vehicles traveling with the flow, so a vehicle-based Lagrangian framework is more appropriate [19, 35, 36].

Consider the highway traffic scenario sketched in Fig. 1(a) with the trajectory of the lead vehicle (black) given. As will be discussed later, this trajectory is used only as boundary condition for traffic simulations, i.e., to generate traffic data for this study, and it does not have to be known by the RSU in practice. We simulate the traffic flow behind the lead vehicle by calculating the position $X(n, t)$ of vehicle n as a function of time t. Note that n is not restricted to integer vehicle numbers. Then the LWR model can be formulated as

$$\partial_t X(n,t) = V(-\partial_n X(n,t)). \tag{1}$$

This model relates the speed $\partial_t X$ to the traffic density $-1/\partial_n X$. The relationship is based on the range policy V which tells the desired speed of vehicles as a function of their distance d from their predecessor (where the distance includes the vehicle length). Here we utilize the range policy

$$V(d) = \begin{cases} 0 & \text{if} \quad d \le d_{\mathrm{st}}, \\ (d - d_{\mathrm{st}})/\tau & \text{if} \quad d_{\mathrm{st}} < d < d_{\mathrm{go}}, \\ v_{\max} & \text{if} \quad d_{\mathrm{go}} \le d. \end{cases} \tag{2}$$

That is, below a standstill distance d_{st} the vehicles intend to stop, above the distance d_{go} the vehicles shall travel at the speed limit $v_{\max}$, and between d_{st} and d_{go} vehicles increase their speed according to a linear function of the distance. The inverse of the gradient of this linear increase is $\tau = (d_{\mathrm{go}} - d_{\mathrm{st}})/v_{\max}$, which can be interpreted as a time gap between subsequent vehicles.

Using the trajectory $X(0, t)$ of the lead vehicle as boundary condition and the equidistant initial spacing $X(n, 0) = X(0, 0) - n(d_{\mathrm{st}} + \tau\, \partial_t X(0, 0))$ of the following vehicles as initial condition, we simulated the LWR model to obtain the traffic flow behind the lead vehicle. Figure 2 shows a simulation where the lead vehicle's trajectory is taken from experimental data, i.e., from the GPS coordinates of a CV traveling in traffic along highway US-39 in Detroit, Michigan; see [19] for details of the experiment. The parameters were set to $d_{\mathrm{st}} = 10\,\mathrm{m}$, $v_{\max} = 40\,\mathrm{m/s}$ and $\tau = 1.5\,\mathrm{s}$, while the total number of simulated follower vehicles is $N = 250$. We refer to these diagrams as space-time plots.

As indicated in Figs. 1 and 2, the LWR model essentially copies the lead vehicle's trajectory and obtains the follower vehicles' trajectories by shifting it in time and space. In fact, the solution of the linear LWR model (that is valid between $d_{\mathrm{st}} < d < d_{\mathrm{go}}$) can be expressed as

$$X(n,t) = X(0, t - n\tau) - n d_{\mathrm{st}}. \tag{3}$$

This is equivalent to Newell's car following model [37] where each vehicle copies the trajectory of its predecessor with a time shift τ and a spatial shift d_{st}; as highlighted in Fig. 1(b). Alternatively, one can also express this relationship

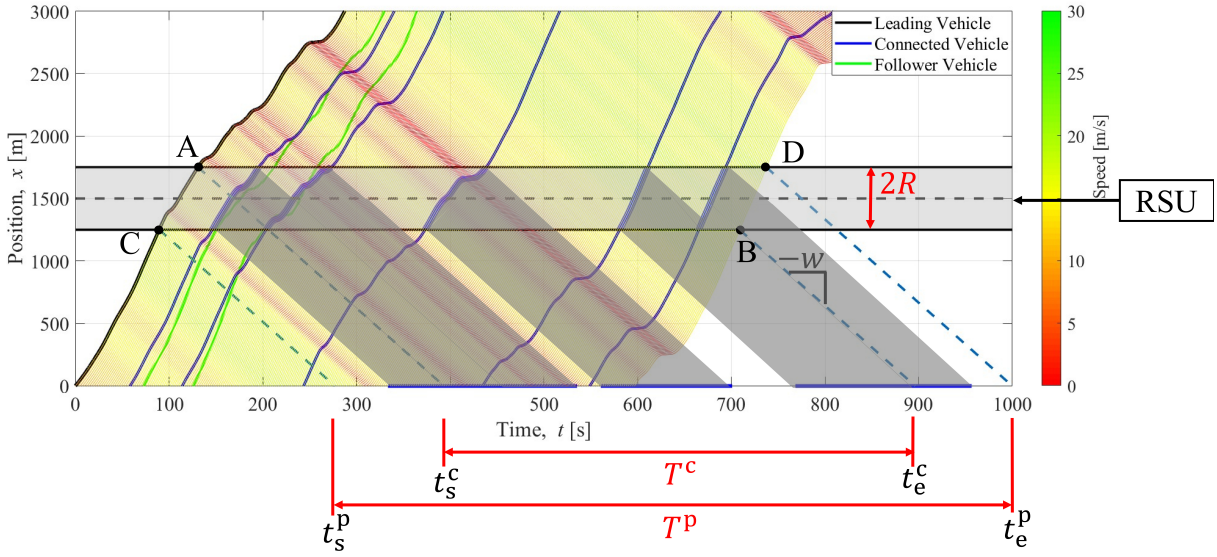

Figure 2: Illustration of the traffic flow on a highway where the measured lead vehicle trajectory is black, measured follower vehicle trajectories are green, the trajectories of simulated vehicles are colored according to their speeds, and connected vehicles are highlighted by blue. A single RSU is located along the road with communication range R as indicated and it provides traffic predictions for location $x = 0$. The duration of the potential coverage zone is indicated by $T^{\mathrm{p}} = t_{\mathrm{e}}^{\mathrm{p}} - t_{\mathrm{s}}^{\mathrm{p}}$, and the duration of the constant coverage zone is indicated by $T^{\mathrm{c}} = t_{\mathrm{e}}^{\mathrm{c}} - t_{\mathrm{s}}^{\mathrm{c}}$. The time intervals covered by predictions are shown by the blue sections.

with the travel time $\mathcal{T}(n, x)$ [35] that represents the time moment when vehicle n reaches location x:

$$\mathcal{T}(n, x) = \mathcal{T}(0, x + nd_{\mathrm{st}}) + n\tau. \tag{4}$$

Note that we have $\mathcal{T}(n, X(n, t)) = t$ and $X(n, \mathcal{T}(n, x)) = x$.

The shifted trajectories in (3) imply that congestion waves propagate upstream along the highway with a constant wave speed $w = d_{\mathrm{st}}/\tau$; see Fig. 1(b). For the parameters chosen we have $w = 6.67\,\mathrm{m/s}$. This provides us with a powerful tool for determining which parts of the traffic (i.e., which regions in space and time) are affected by a certain CV's motion. This will help us evaluate the availability (coverage) of traffic predictions for different penetration rates of CVs and placements of the RSUs along the highway. The analysis below is based on the simulated traffic patterns in Fig. 2 and we utilize the constant wave speed assumption for traffic predictions. The quality of traffic prediction by the LWR model can be seen from the comparison of measured follower trajectories (green) and selected simulated CV trajectories (blue). Even though the lead and follower vehicles were on different lanes of the highway during the experiment, the simulation captures the real follower vehicles' motion well. We remark that while traffic predictions can be done by other, more sophisticated models as well (such as the ones in [38, 39, 40, 41, 42, 43]), the regions where traffic predictions are available in space and time are well-captured by the constant wave speed assumption.

4. Traffic Predictions by a Single Roadside Unit

In this section, we focus on the case where information from a single RSU is available. We derive the time interval over which traffic predictions can potentially be provided by the RSU for vehicles passing a certain location of interest along the road. We call this time interval as *potential coverage zone*. Predictions, however, will only be provided if there are CVs passing through the communication range of the RSU with sufficient penetration in the traffic flow. When predictions are available, we say that the corresponding region in space-time is *covered* by predictions. Then, we introduce the so-called *coverage rate* and *total time covered* as metrics to characterize how large portion of the space-time the RSU can cover by predictions.

4.1. Potential Coverage Zone

Consider the scenario in Fig. 2 which shows the simulated traffic flow (colored area) with $N = 250$ follower vehicles (251 total vehicles). Assume that an RSU is operating at location x_{RSU} (shown by black dashed line at $x_{\mathrm{RSU}} = 1500\,\mathrm{m}$), and it is monitoring traffic within its communication range via connectivity. If the communication range of the RSU is R, then it can detect vehicles on a road segment of length $2R$ (indicated by the light gray shaded region between two black lines for $2R = 500\,\mathrm{m}$). This way the RSU can monitor vehicles over a certain duration of time and provide traffic predictions for certain regions in space-time, as described below.

Imagine the case when the RSU has the information of all vehicles inside its communication range. Then the *potential coverage zone* is the time interval $t \in [t_{\mathrm{s}}^{\mathrm{p}}, t_{\mathrm{e}}^{\mathrm{p}}]$ when predictions can be received from the RSU at a location x of interest; see Fig. 2. Here we focus on predictions upstream the RSU only by assuming $x < x_{\mathrm{RSU}} - R$. According to the constant wave speed assumption, the potential coverage zone lies between the characteristic lines of slope $-w$ indicated by dashed blue lines in Fig. 2. The leftmost characteristic line emanates from point C where the lead vehicle 0 enters the RSU's range at time $\mathcal{T}(0, x_{\mathrm{RSU}} - R)$, whereas the rightmost characteristic line emanates from point D where the trajectory of the last vehicle N exits the RSU's range at time $\mathcal{T}(N, x_{\mathrm{RSU}} + R)$. According to Fig. 2 and (4), the potential coverage zone can be obtained by expressing $t_{\mathrm{s}}^{\mathrm{p}}$ and $t_{\mathrm{e}}^{\mathrm{p}}$ from the following equations:

$$\begin{aligned} t_{\mathrm{s}}^{\mathrm{p}} - \frac{x_{\mathrm{RSU}} - R - x}{w} &= \mathcal{T}(0, x_{\mathrm{RSU}} - R), \\ t_{\mathrm{e}}^{\mathrm{p}} - \frac{x_{\mathrm{RSU}} + R - x}{w} &= \mathcal{T}(N, x_{\mathrm{RSU}} + R) = \mathcal{T}(0, x_{\mathrm{RSU}} + R + Nd_{\mathrm{st}}) + N\tau. \end{aligned} \tag{5}$$

Using $w = d_{\mathrm{st}}/\tau$, the duration of the potential coverage zone becomes

$$T^{\mathrm{p}}(x_{\mathrm{RSU}}) = t_{\mathrm{e}}^{\mathrm{p}} - t_{\mathrm{s}}^{\mathrm{p}} = \mathcal{T}(0, x_{\mathrm{RSU}} + R + Nd_{\mathrm{st}}) - \mathcal{T}(0, x_{\mathrm{RSU}} - R) + (Nd_{\mathrm{st}} + 2R)\frac{1}{w}. \tag{6}$$

Here we emphasize that the duration T^{p} depends on the location x_{RSU} of the RSU, the number of vehicles $(N + 1)$ monitored, and on the traffic conditions (i.e., how the travel time $\mathcal{T}$ changes along the highway), while it is independent of the location x of interest. These will be important when suggesting a deployment strategy.

Formula (6) contains the travel time of the lead vehicle. This may be estimated using the average speed of this vehicle. In particular, consider the case where the lead vehicle drives with approximately constant speed, i.e., $X(0, t) \approx vt$ and, equivalently, $\mathcal{T}(0, x) \approx x/v$. The constant speed assumption eliminates the dependence on the traffic conditions and the RSU's location by reducing (6) to

$$T^{\mathrm{p}} \approx (Nd_{\mathrm{st}} + 2R)\left(\frac{1}{v} + \frac{1}{w}\right). \tag{7}$$

For example, an estimate of the average speed in Fig. 2 is $v \approx 11\,\mathrm{m/s}$ which leads to the estimate $T^{\mathrm{p}} \approx 723\,\mathrm{s}$. Although this simplification eliminates the location dependency for a single RSU, it will be useful in the next section where we consider two RSUs and establish a simple relationship between the distance of the RSUs and coverage.

The duration T^{p} of the potential coverage zone was calculated numerically for various RSU locations using (6) as plotted by the green curve in Fig. 3(a). It can be observed that T^{p} has a small (about 5%) fluctuation around its estimated value (7) shown by the dashed brown line. The value of T^{p} is plotted against the number of follower vehicles in Fig. 3(b). This figure demonstrates that T^{p} increases monotonically with the number of vehicles, i.e., monitoring more vehicles increases the amount of potentially available traffic predictions. These conclusions are supported by (6), since the travel time $\mathcal{T}$ monotonically increases with respect to its second argument, and thus T^{p} monotonically increases with N. It should also be noted from Fig. 3(b) that there is a considerable potential coverage zone (> 100 s) even for a single vehicle.

Now consider an arbitrary point within the potential coverage zone, and consider the characteristic line passing through it. This point may potentially receive a prediction based on those pieces of vehicle trajectories that lie within the RSU's range and are crossed by the characteristic line. In a certain part of the potential coverage zone the number of such trajectories is constant, namely $2R/d_{\mathrm{st}}$. We call this region as *constant coverage zone* and denote it by $t \in [t_{\mathrm{s}}^{\mathrm{c}}, t_{\mathrm{e}}^{\mathrm{c}}]$; see Fig. 2. This zone is located between two characteristic lines: the left one emanates from point A where the lead

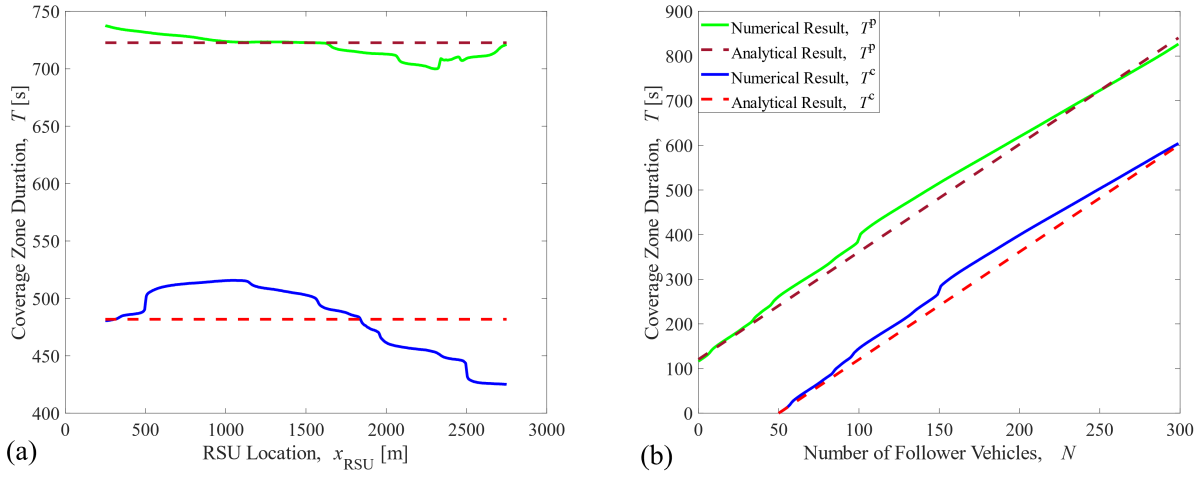

Figure 3: The duration of the potential and constant coverage zones as function of (a) the RSU location x_{RSU} (when $N = 250$) and (b) the number N of follower vehicles (when $x_{\mathrm{RSU}} = 1500\,\mathrm{m}$) for the setup illustrated in Fig. 2. Both panels compare the exact numerical results given by (6) and (8) to the approximate analytical results obtained from (7) and (9) that use constant speed approximation (with $v = 11\,\mathrm{m/s}$).

vehicle 0 exits the RSU's range, whereas the right one emanates from point B where the last vehicle N enters the RSU's range. Similarly to (7), the duration of the constant coverage zone can be determined by

$$T^{\mathrm{c}}(x_{\mathrm{RSU}}) = t_{\mathrm{e}}^{\mathrm{c}} - t_{\mathrm{s}}^{\mathrm{c}} = \mathcal{T}\,(0, x_{\mathrm{RSU}} - R + Nd_{\mathrm{st}}) - \mathcal{T}\,(0, x_{\mathrm{RSU}} + R) + (Nd_{\mathrm{st}} - 2R)\,\frac{1}{w}. \tag{8}$$

Notice the sign change of the R terms compared to the formula of T^{p}. Using the average speed v, this can be approximated by

$$T^{\mathrm{c}} \approx (Nd_{\mathrm{st}} - 2R)\left(\frac{1}{v} + \frac{1}{w}\right). \tag{9}$$

For example, an average speed of $v \approx 11\,\mathrm{m/s}$ leads to the estimate $T^{\mathrm{c}} \approx 482\,\mathrm{s}$.

The duration T^{c} of the constant coverage zone is plotted against the RSU's location and the number of vehicles in Fig. 3(a) and (b); see the blue curves computed based on (8) and the red dashed lines obtained from (9). Fig. 3(b) demonstrates that T^{c} increases monotonically with the number of vehicles, similarly to the trend of T^{p}. Additionally, according to (8) and Fig. 3(b), the number N of follower vehicles has to be larger than $2R/d_{\mathrm{st}}$ (which is 50 vehicles in our example) to ensure $T^{\mathrm{c}} > 0$. Note that, however, that this is only needed to ensure the existence of the constant coverage zone which is defined to perform the analysis below. For the potential coverage zone, on the other hand, we still have $T^{\mathrm{p}} > 0$ even for a single vehicle.

4.2. Coverage Rate and Total Time Covered

Up to this point, we considered the ideal case where the RSU has the information of all vehicles inside its communication range. In reality, the RSU only has access to the information of connected vehicles (CVs) equipped with V2X devices. Consider Fig. 2 and assume that only some of the vehicles are CVs (blue trajectories). The CVs may be human-driven or possess different levels of automation. The number of CVs in traffic is characterized by the *penetration rate* λ. In particular, we assume that connected vehicles are uniformly and randomly distributed among all vehicles, and the probability of a vehicle to be connected is the penetration rate λ. As a result, the connectivity of vehicles can be considered as a Poisson point process: when enumerating the vehicles from upstream to downstream, the event that a vehicle is connected has the same probability for each individual vehicle independent of other vehicles. Furthermore, we assume that the penetration rate is approximately constant over the duration of our experiment. Note, however, that our results are applicable to any penetration level at any hour of the day. For a penetration rate λ,

the number of CVs approaches λN for large N. Fig. 2 shows an example where vehicles are selected to be connected with penetration rate $\lambda = 2\%$.

Once the RSU monitors the trajectories of the CVs within its range, it can provide traffic predictions for certain points of the potential coverage zone (see the horizontal blue lines in Fig. 2). These points are determined by the projection of the CV trajectories along the characteristic direction (see gray shading). An arbitrary point inside the potential coverage zone may receive a prediction if its characteristic line crosses at least one CV trajectory within the RSU's range. If a point receives a prediction, we say the point is covered. To indicate coverage, we use the indicator function $\mathbb{1}_{\mathrm{cov}}(t)$ that gives 1 when time t is covered and 0 otherwise. Coverage has a certain probability that depends on the probability of the corresponding vehicles being connected. As shown later, points inside the constant coverage zone have the same probability of being covered because the number of vehicles that can potentially provide predictions is the same.

To quantify coverage, we now define the *total time covered* T_{tot} as the expected duration of coverage over a selected interval $t \in [t_{\mathrm{s}}, t_{\mathrm{e}}]$:

$$T_{\mathrm{tot}} = \mathbb{E}\left[\int_{t_{\mathrm{s}}}^{t_{\mathrm{e}}} \mathbb{1}_{\mathrm{cov}}(t)\mathrm{d}t\right]. \tag{10}$$

This is a useful metric to determine where the RSU shall be located to maximize the amount of available predictions. From this, the definition of the *coverage rate* follows naturally, which is the expected coverage of the points in the selected time horizon:

$$C = \mathbb{E}\left[\frac{1}{t_{\mathrm{e}} - t_{\mathrm{s}}}\int_{t_{\mathrm{s}}}^{t_{\mathrm{e}}} \mathbb{1}_{\mathrm{cov}}(t)\mathrm{d}t\right]. \tag{11}$$

These definitions can be used for both the potential coverage zone:

$$T^{\mathrm{p}}_{\mathrm{tot}} = \mathbb{E}\left[\int_{t^{\mathrm{p}}_{\mathrm{s}}}^{t^{\mathrm{p}}_{\mathrm{e}}} \mathbb{1}_{\mathrm{cov}}(t)\mathrm{d}t\right], \qquad C^{\mathrm{p}} = \mathbb{E}\left[\frac{1}{T^{\mathrm{p}}}\int_{t^{\mathrm{p}}_{\mathrm{s}}}^{t^{\mathrm{p}}_{\mathrm{e}}} \mathbb{1}_{\mathrm{cov}}(t)\mathrm{d}t\right], \tag{12}$$

and the constant coverage zone:

$$T^{\mathrm{c}}_{\mathrm{tot}} = \mathbb{E}\left[\int_{t^{\mathrm{c}}_{\mathrm{s}}}^{t^{\mathrm{c}}_{\mathrm{e}}} \mathbb{1}_{\mathrm{cov}}(t)\mathrm{d}t\right], \qquad C^{\mathrm{c}} = \mathbb{E}\left[\frac{1}{T^{\mathrm{c}}}\int_{t^{\mathrm{c}}_{\mathrm{s}}}^{t^{\mathrm{c}}_{\mathrm{e}}} \mathbb{1}_{\mathrm{cov}}(t)\mathrm{d}t\right]. \tag{13}$$

We use both numerical and analytical calculations to evaluate these quantities. To obtain the total time covered and coverage rate numerically, we select some of the vehicles to be connected based on uniform random distribution, where the probability of being connected is given by the penetration rate λ. Then, we consider those parts of the CV trajectories that lie inside the RSU's communication range (thick blue), and project these parts to the time axis as indicated in Fig. 2. This projection implies coverage for the dark gray shaded space-time regions, and consequently, the blue domain at the location of interest. The indicator function $\mathbb{1}_{\mathrm{cov}}(t)$ is equal to 1 in this blue domain and 0 outside. Then, we can calculate the total time covered and coverage rate with (12) and (13). We repeat this calculation 10000 times by randomly reassigning the CVs each time, and we average the results to obtain an approximation of the expected value.

While analytical expressions for C^{p} are hard to obtain, the definition of the constant coverage zone leads to a simple formula for C^{c} as given below. We refer to C^{c} as the *constant coverage rate*. Consider an arbitrary point inside the constant coverage zone and draw a characteristic line through this point. The number of vehicle trajectories crossed by the characteristic line within the RSU's communication range is $2R/d_{\mathrm{st}}$, irrespective of which point we consider in the constant coverage zone. The probability of the selected point to be covered is equal to the probability of at least one of these $2R/d_{\mathrm{st}}$ subsequent vehicles to be connected. Since this probability is the same regardless of which point we choose, the constant coverage rate C^{c} is equal to the probability of an arbitrary point to be covered in the constant coverage zone. To calculate this probability, we go through the $2R/d_{\mathrm{st}}$ subsequent vehicles from upstream to downstream and we sum the probabilities that a vehicle is connected while other vehicles upstream are not connected. As the connectivity of each vehicle is a Poisson process, the probability that the m-th vehicle is connected while

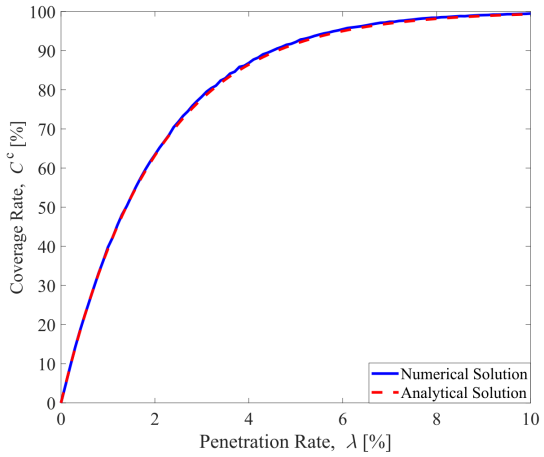

Figure 4: Numerical and analytical results for the constant coverage rate as a function of the penetration rate for a single RSU with communication range $R = 250$ m.

Table 2: The constant coverage rate of a single RSU at different penetration rates and RSU communication ranges.

RSU Range, R / Penetration Rate, λ	100m	250m	500m
2%	33%	63%	86%
5%	63%	92%	99%
10%	86%	99%	99.99%

vehicles upstream are not connected is the time between events of the Poisson process, thus equals $\lambda e^{-\lambda m}$ according to the exponential distribution. Therefore, the constant coverage rate C^c can be calculated as

$$C^c = \int_0^{2R/d_{st}} \lambda e^{-\lambda m} dm = 1 - e^{-\lambda \frac{2R}{d_{st}}}, \tag{14}$$

where a continuum of vehicles was assumed when using integral instead of a sum. Note that C^c is determined by the penetration rate of CVs and the communication range of the RSU, while it depends neither on the RSU location nor on the traffic conditions.

The numerical and analytical results for the constant coverage rate C^c as a function of the penetration rate are plotted in Fig. 4 by solid blue and dashed red lines, respectively. Notice the remarkable agreement between the numerical and analytical results. Since the constant coverage rate is affected by the penetration rate of connectivity, it may not reach 100%. However, the figure demonstrates that the constant coverage rate C^c approaches 100% exponentially as the penetration rate is increased. Therefore, equipping more vehicles with V2X communication devices can lead to significant benefits, and even a few percents of penetration can already achieve high coverage. Increasing the RSU's communication range can further improve the constant coverage rate C^c, although this requires improving the roadside infrastructure. The constant coverage rate values for some representative penetration rates and communication ranges are listed in Table 2.

Based on the constant coverage rate C^c and the duration T^c, we can obtain the total time covered T^c_{tot}. Furthermore,

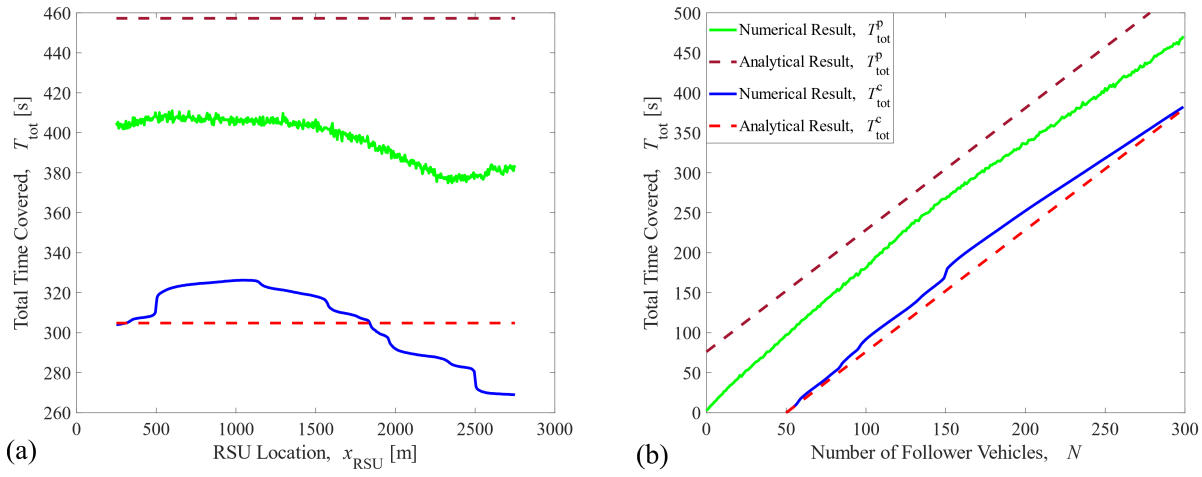

Figure 5: The total time covered for the potential and constant coverage zones as function of (a) the RSU location x_{RSU} (when $N = 250$) and (b) the number N of follower vehicles (when $x_{\text{RSU}} = 1500\,\text{m}$) for the setup illustrated in Fig. 2. The CV penetration rate is set to $\lambda = 2\%$. Both panels compare the exact numerical results given by (12) and (13) to the approximate analytical results obtained from (15) that uses constant speed approximation (with $v = 11\,\text{m/s}$).

using C^{c} and T^{p} we get an over-approximation of $T^{\text{p}}_{\text{tot}}$:

$$\begin{aligned} T^{\text{c}}_{\text{tot}}(x_{\text{RSU}}) = C^{\text{c}}T^{\text{c}}(x_{\text{RSU}}) &= \left(1-\mathrm{e}^{-\lambda\frac{2R}{d_{\text{st}}}}\right)\left(\mathcal{T}\left(0, x_{\text{RSU}}-R+Nd_{\text{st}}\right)-\mathcal{T}\left(0, x_{\text{RSU}}+R\right)+\left(Nd_{\text{st}}-2R\right)\frac{1}{w}\right) \\ &\approx \left(1-\mathrm{e}^{-\lambda\frac{2R}{d_{\text{st}}}}\right)\left(Nd_{\text{st}}-2R\right)\left(\frac{1}{v}+\frac{1}{w}\right), \\ T^{\text{p}}_{\text{tot}}(x_{\text{RSU}}) \le C^{\text{c}}T^{\text{p}}(x_{\text{RSU}}) &= \left(1-\mathrm{e}^{-\lambda\frac{2R}{d_{\text{st}}}}\right)\left(\mathcal{T}\left(0, x_{\text{RSU}}+R+Nd_{\text{st}}\right)-\mathcal{T}\left(0, x_{\text{RSU}}-R\right)+\left(Nd_{\text{st}}+2R\right)\frac{1}{w}\right) \\ &\approx \left(1-\mathrm{e}^{-\lambda\frac{2R}{d_{\text{st}}}}\right)\left(Nd_{\text{st}}+2R\right)\left(\frac{1}{v}+\frac{1}{w}\right), \end{aligned} \tag{15}$$

cf. (6)-(9) and (14). Compared to $T^{\text{p}}_{\text{tot}}$, $T^{\text{c}}_{\text{tot}}$ neglects the predictions outside the constant coverage zone but inside the potential coverage zone. For a large number of vehicles monitored, the relative difference between these two metrics becomes negligibly small.

The numerical and analytical results for $T^{\text{p}}_{\text{tot}}$ and $T^{\text{c}}_{\text{tot}}$ are shown in Fig. 5 for CV penetration rate $\lambda = 2\%$. Fig. 5(a) highlights that the metrics $T^{\text{p}}_{\text{tot}}$ and $T^{\text{c}}_{\text{tot}}$ depend on the location of the RSU and follow a similar trend. Therefore, either one of these metrics can be used to determine the optimal RSU placement and guide RSU deployment, while $T^{\text{c}}_{\text{tot}}$ is easier to analyze. In our single RSU example, the total time covered $T^{\text{c}}_{\text{tot}}$ is maximized in the congested region around $x_{\text{RSU}} \approx 1100\,\text{m}$. This indicates the optimal placement of a single RSU. Meanwhile Fig. 5(b) indicates that the total time covered increases monotonically with the number of vehicles monitored. This may reflect requirements on how many vehicles need to be monitored in order to avoid a certain level of coverage.

5. Sparse Deployment of Multiple Roadside Units

The deployment of multiple RSUs is a critical concern for establishing a connected highway infrastructure. In this section, we first analyze a baseline for multiple RSU deployment, then we propose a sparse RSU deployment strategy and compare it with the baseline. We investigate how the distance between two RSUs affects the prediction capability if their mean position is fixed. This allows one to decide the optimal distance between RSUs and thus sequentially determine the placement of multiple RSUs along an instrumented highway segment. We use a reasonable assumption

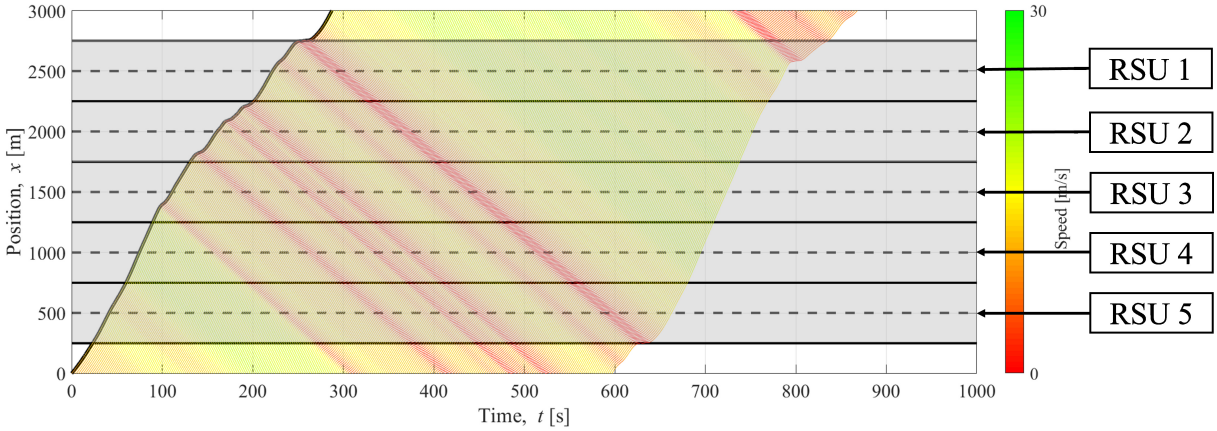

Figure 6: Baseline scenario for multiple RSU deployment where five RSUs are located such that any point along a road segment lies within the communication range of one of the RSUs.

that the RSUs have the same communication range R. In addition to the parameters of the previous section, the distance D between the RSUs will be considered when developing the sparse RSU deployment strategy.

Before proposing our strategy, we introduce a baseline method for deploying multiple RSUs, shown in Fig. 6. In this baseline, RSUs are placed such that the boundaries of their communication ranges coincide, creating a dense network of RSUs along the highway. This method allows communication between the infrastructure and the CVs anywhere on the instrumented highway segment, although it requires a large number of RSUs implying large instrumentation and maintenance costs. As an example, consider the setup of five RSUs in Fig. 6, each with range $R = 250\,\text{m}$, that provides V2I connectivity from 250 m to 2750 m along the road. Numerical results show that this setup has a potential coverage zone of duration $T^{\text{p}} = 1183\,\text{s}$ and a total time covered $T^{\text{p}}_{\text{tot}} = 947\,\text{s}$ with a penetration rate of 2%. These will be used to make comparison with our proposed sparse RSU deployment strategy discussed below.

5.1. Critical Distance and Potential Coverage Zones

In an effort to reduce the RSU deployment cost (i.e., the number of RSUs) while maintaining large coverage (i.e., potential coverage zone and total time covered), we focus on the deployment of two RSUs in the rest of the paper. Nevertheless, the results of the two-RSU deployment can be easily extended to the deployment of more, sparsly distributed RSUs along the road by the help of the metrics proposed in Sec. 4.

Consider the two-RSU setup in Fig. 7, where the locations of the RSUs are $x_1 \geq x_2$ and their distance is $D = x_1 - x_2$. For a given number of simulated vehicles (e.g., $N + 1 = 251$), the potential and constant coverage zones can be determined for each individual RSU separately, according to Sec. 4. We denote the durations of the constant coverage zones by T^{c}_1 and T^{c}_2. If the distance D of the two RSUs is large enough, the two time zones have no overlap and the problem reduces to two separate single RSU cases discussed in Sec. 4; see the illustration in Fig. 7(a). Note that in this case there is a region between the individual coverage zones where traffic prediction cannot be provided by any of the RSUs. At a critical distance $D = D_{\text{c}}$ the individual coverage zones "touch" each other as illustrated in Fig. 7(b). When the distance D is less than the critical D_{c}, there exists a time zone of duration T^{c}_{12} that can potentially be covered by predictions via both RSU; see Fig. 7(c). Here we first calculate the critical distance, and then we analyze the constant coverage rate and the total time covered for $D \leq D_{\text{c}}$.

We calculate the critical distance D_{c} by formulating the duration T^{c}_{12} of the double-covered time zone and taking $T^{\text{c}}_{12} = 0$. Similar to (8), we can write

$$T^{\text{c}}_{12} = \begin{cases} \mathcal{T}\left(0, x_2 - R + Nd_{\text{st}}\right) - \mathcal{T}\left(0, x_1 + R\right) + \left(Nd_{\text{st}} - 2R - D\right)\frac{1}{w} & \text{if} \quad 0 \leq D \leq D_{\text{c}}, \\ 0 & \text{if} \quad D > D_{\text{c}}. \end{cases} \tag{16}$$

For the critical distance the travel times in the top row are equal (cf. Fig. 7(b)), and consequently, $T^{\text{c}}_{12} = 0$ yields

$$D_{\text{c}} = Nd_{\text{st}} - 2R. \tag{17}$$

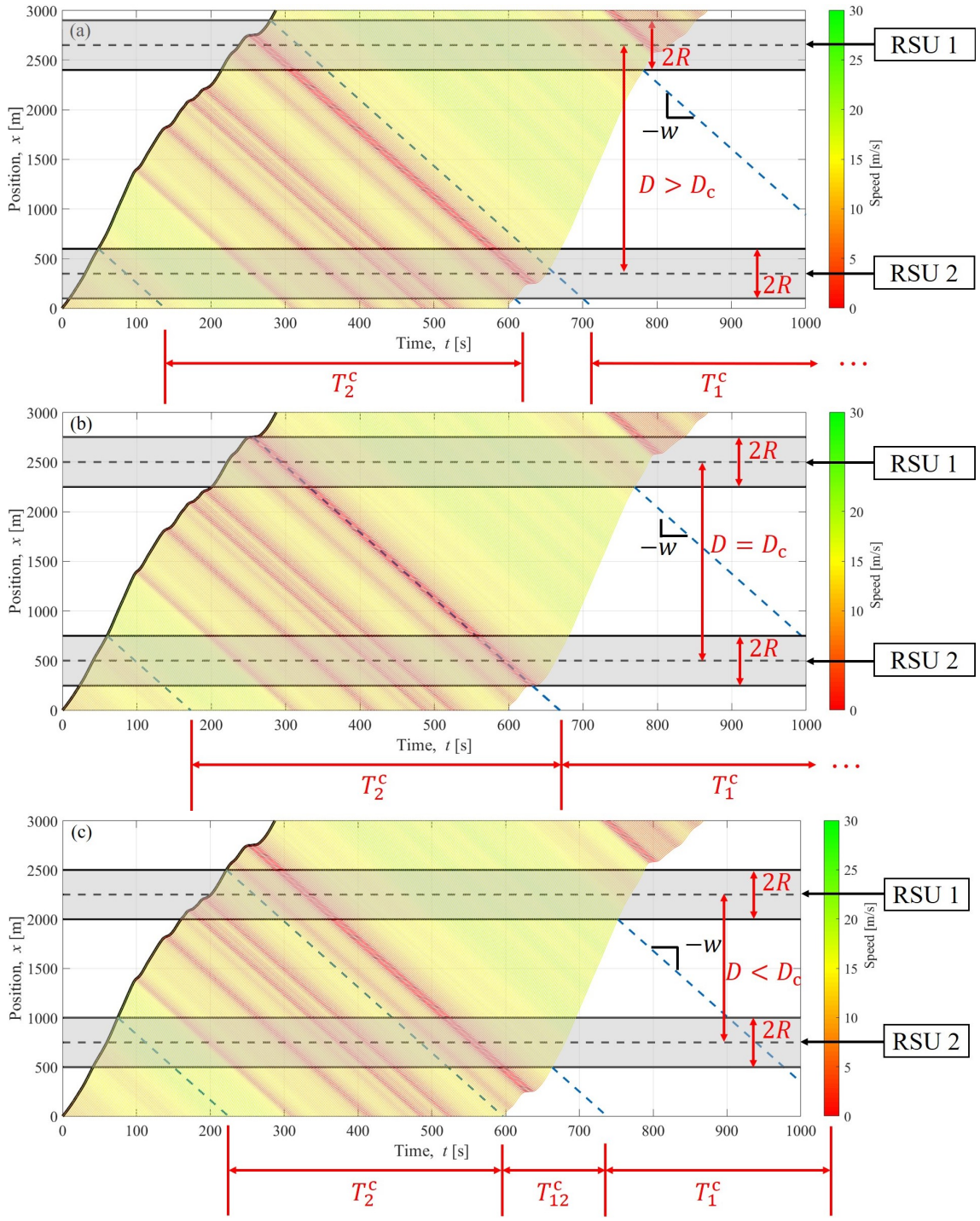

Figure 7: Setup with two RSUs where the distance of the RSUs is (a) larger than the critical distance $D > D_c$, (b) equal to the critical distance $D = D_c$ and (c) smaller than the critical distance $D < D_c$.

Note that D_c depends only on the number $(N + 1)$ of vehicles monitored, the standstill distance d_{st} and the RSU's communication range R. This implies a trade-off between monitoring more vehicles ($(N + 1)$) and placing the RSUs farther apart (D_c). Meanwhile, neither the RSU locations nor the traffic conditions affect the value of D_c. Furthermore,

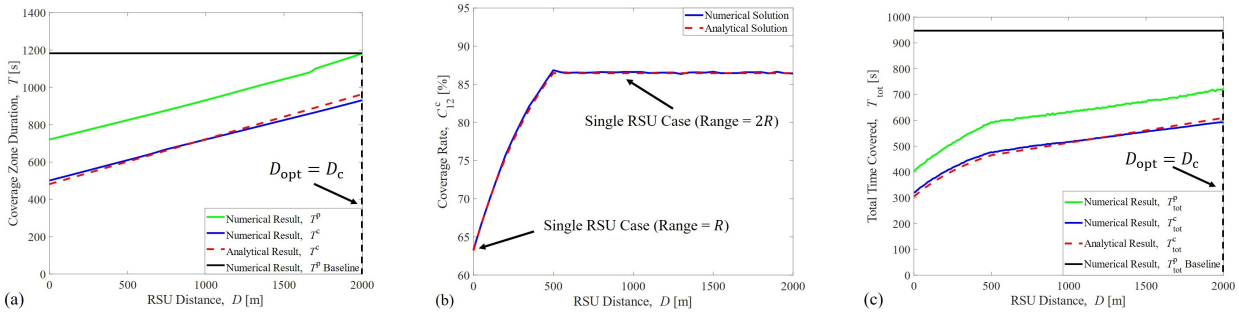

Figure 8: (a) The duration of the potential and constant coverage zones for two RSUs as a function of their distance. (b) Coverage rate C^{c}_{12} as a function of RSU distance. (c) The total time covered by two RSUs as a function of their distance. The parameters are $R = 250\,\text{m}$ and $\lambda = 2\%$. The mean position of the two RSUs is fixed to the location $x = 1500\,\text{m}$. The exact numerical results of T^{p} and $T^{\text{c}}_{\text{tot}}$ given by (6) and (10) are compared to the approximate analytical results obtained by variants of (7) and (23) that use constant speed approximation (with $v = 11\,\text{m/s}$). The exact numerical results for the baseline are also shown for comparison.

we assume that a sufficient number of vehicles ($N > 2R/d_{\text{st}}$) is monitored so that the critical distance is positive. In the example of Fig. 7 the critical distance is $D_{\text{c}} = 2000\,\text{m}$. Based on T^{c}_{12}, the durations of the time zones which can be covered by one of the RSUs only are

$$\begin{aligned} T^{\text{c}}_1 &= T^{\text{c}}(x_1) - T^{\text{c}}_{12}, \\ T^{\text{c}}_2 &= T^{\text{c}}(x_2) - T^{\text{c}}_{12}, \end{aligned} \tag{18}$$

where $T^{\text{c}}(x_1)$ and $T^{\text{c}}(x_2)$ are given by formula (8) derived for a single RSU.

Considering the union of the coverage zones, Fig. 8(a) plots the duration $T^{\text{p}}_1 + T^{\text{p}}_2 + T^{\text{p}}_{12}$ of the potential coverage zone (green) and the duration $T^{\text{c}}_1 + T^{\text{c}}_2 + T^{\text{c}}_{12}$ of the constant coverage zone (red and blue) as a function of the distance D. The result for the baseline method with five RSUs is also indicated (black). It can be observed that the duration of the potential coverage zone for two RSUs approaches the one for the five-RSU baseline as D approaches $D_{\text{c}} = 2000\,\text{m}$. This indicates that the same potential coverage zone can be achieved with significantly less RSUs if the number of vehicles monitored is large enough.

5.2. Coverage Rate and Optimal RSU Distance Based on Total Time Covered

Now we calculate the constant coverage rates C^{c}_1, C^{c}_2 and C^{c}_{12} of the three time zones associated with T^{c}_1, T^{c}_2 and T^{c}_{12}, respectively, while assuming $D \le D_{\text{c}}$. The coverage rates $C^{\text{c}}_1 = C^{\text{c}}_2 = C^{\text{c}}$ of the regions covered by a single RSU only can be calculated from (14), while the coverage rate C^{c}_{12} related to both RSUs is derived below, by following the analysis presented for the single RSU setup.

We distinguish two scenarios: (i) when $0 \le D \le 2R$ and (ii) when $D > 2R$. When $0 \le D \le 2R$ the communication ranges of the two RSUs intersect, and this case can be considered as a single RSU setup with the larger range $D + 2R$, i.e., the union of the ranges of the two RSUs. Therefore, C^{c}_{12} can be calculated by (14) using the communication range $D + 2R$ instead of $2R$. When $D > 2R$, the communication ranges of the two RSUs no longer intersect. Based on the discussion about the coverage rate of a single RSU, there is a certain set of vehicles for each RSU that can potentially provide prediction for an arbitrary point in the zone of duration T^{c}_{12}. For two RSUs the number of vehicles to potentially provide coverage is doubled compared to the single RSU case. Therefore, (14) applies with the exponent $4R/d_{\text{st}}$ instead of $2R/d_{\text{st}}$. The expression of C^{c}_{12} is summarized as

$$C^{\text{c}}_{12} = \begin{cases} 1 - \text{e}^{-\lambda \frac{2R+D}{d_{\text{st}}}}, & \text{if} \quad 0 \le D \le 2R, \\ 1 - \text{e}^{-\lambda \frac{4R}{d_{\text{st}}}}, & \text{if} \quad D > 2R. \end{cases} \tag{19}$$

The coverage rates of three or more RSUs could be derived analogously.

The analytical result (19) for the coverage rate C^{c}_{12} is plotted as a function of the distance D in Fig. 8(b), together with its numerical counterpart based on (11). From point of view of predictions, the two RSUs function as a single RSU when they are at the same location, and thus, C^{c}_{12} is minimal for $D = 0$. As the RSUs are moved apart, the

coverage rate C^{c}_{12} increases. Once the RSUs are at a distance greater than two times their communication range ($D > 2R$), the coverage rate saturates at a level $C^{\mathrm{c}}_{12,\max}$ that is equal to the coverage rate of a single RSU with doubled communication range. Finally, it is important to note that the coverage rate $C^{\mathrm{c}}_{12,\max}$ associated with two RSUs is smaller than twice of the coverage rate C^{c} of a single RSU. This can be shown by

$$2C^{\mathrm{c}} - C^{\mathrm{c}}_{12} \geq 2C^{\mathrm{c}} - C^{\mathrm{c}}_{12,\max} = 2\left(1 - \mathrm{e}^{-\lambda\frac{2R}{d_{\mathrm{st}}}}\right) - \left(1 - \mathrm{e}^{-\lambda\frac{4R}{d_{\mathrm{st}}}}\right) = \left(1 - \mathrm{e}^{-\lambda\frac{2R}{d_{\mathrm{st}}}}\right)^2 > 0. \tag{20}$$

This observation implies that it is more efficient to cover different time zones with the two RSUs instead of double-covering a single region. This will be important in terms of finding the optimal distance of the RSUs, which is discussed below.

To calculate the optimal RSU distance, we calculate the total time covered $T^{\mathrm{c}}_{\mathrm{tot}}$:

$$T^{\mathrm{c}}_{\mathrm{tot}} = T^{\mathrm{c}}_1 C^{\mathrm{c}}_1 + T^{\mathrm{c}}_2 C^{\mathrm{c}}_2 + T^{\mathrm{c}}_{12} C^{\mathrm{c}}_{12}, \tag{21}$$

cf. (15). Here, T^{c}_1, T^{c}_2, and T^{c}_{12} can be obtained from (8) and (16), while C^{c}_1, C^{c}_2 and C^{c}_{12} can be calculated from (14) and (19). Maximizing the value of $T^{\mathrm{c}}_{\mathrm{tot}}$ yields the optimum RSU deployment in terms of achieving the largest amount of traffic predictions from the RSUs.

Now we derive the optimal distance D_{opt} between the two RSUs that maximizes the total time covered $T^{\mathrm{c}}_{\mathrm{tot}}$ for the case $D \leq D_{\mathrm{c}}$. First, we derive D_{opt} for the simplest case where the lead vehicle drives with approximately constant speed, i.e., its motion is given by $X(0,t) \approx vt$, or equivalently, $\mathcal{T}(0,x) \approx x/v$. Then, the duration of the potential coverage zones given by (16) and (18) simplify to

$$\begin{aligned} T^{\mathrm{c}}_{12} &\approx \left(\frac{1}{v} + \frac{1}{w}\right)(D_{\mathrm{c}} - D), \\ T^{\mathrm{c}}_1 \approx T^{\mathrm{c}}_2 &\approx \left(\frac{1}{v} + \frac{1}{w}\right)D, \end{aligned} \tag{22}$$

cf. (9). With $C^{\mathrm{c}}_1 = C^{\mathrm{c}}_2 = C^{\mathrm{c}}$, (21) and (22) lead to the total time covered:

$$\begin{aligned} T^{\mathrm{c}}_{\mathrm{tot}} &\approx \left(\frac{1}{v} + \frac{1}{w}\right)\left((2C^{\mathrm{c}} - C^{\mathrm{c}}_{12})D + C^{\mathrm{c}}_{12} D_{\mathrm{c}}\right) \\ &= \begin{cases} \left(\frac{1}{v} + \frac{1}{w}\right)\left((1 + \mathrm{e}^{-\lambda\frac{2R+D}{d_{\mathrm{st}}}} - 2\mathrm{e}^{-\lambda\frac{2R}{d_{\mathrm{st}}}})D + (1 - \mathrm{e}^{-\lambda\frac{2R+D}{d_{\mathrm{st}}}})(Nd_{\mathrm{st}} - 2R)\right), & \text{if} \quad 0 \leq D \leq 2R, \\ \left(\frac{1}{v} + \frac{1}{w}\right)\left((1 + \mathrm{e}^{-\lambda\frac{4R}{d_{\mathrm{st}}}} - 2\mathrm{e}^{-\lambda\frac{2R}{d_{\mathrm{st}}}})D + (1 - \mathrm{e}^{-\lambda\frac{4R}{d_{\mathrm{st}}}})(Nd_{\mathrm{st}} - 2R)\right), & \text{if} \quad D > 2R. \end{cases} \end{aligned} \tag{23}$$

Since $2C^{\mathrm{c}} - C^{\mathrm{c}}_{12}$ is positive according to (20), the total time covered $T^{\mathrm{c}}_{\mathrm{tot}}$ monotonously increases as a function of the distance D. Therefore, for constant speeds, the optimal deployment strategy is putting the two RSUs at the largest possible distance that is the critical distance $D_{\mathrm{opt}} = D_{\mathrm{c}}$.

For non-constant speed, the total time covered $T^{\mathrm{c}}_{\mathrm{tot}}$ is affected by the trajectory of the lead vehicle through (8) and (16). Still, the average speed of this vehicle can be used in (23) for approximate analytical results. Figure 8(c) shows these analytical results (red) for $T^{\mathrm{c}}_{\mathrm{tot}}$ as a function of the distance D in the range $0 \leq D \leq D_{\mathrm{c}}$. Here the mean position of the two RSUs is fixed to the location $x = 1500\,\mathrm{m}$, and the approximation (23) uses the average speed $v = 11\,\mathrm{m/s}$. Furthermore, numerical results for $T^{\mathrm{c}}_{\mathrm{tot}}$ (blue) and $T^{\mathrm{p}}_{\mathrm{tot}}$ (green) based on (10) are also indicated. Notice the agreement between the analytical and numerical results, and note that the trends of $T^{\mathrm{c}}_{\mathrm{tot}}$ and $T^{\mathrm{p}}_{\mathrm{tot}}$ are the same. This shows that the analytical formula (23) for $T^{\mathrm{c}}_{\mathrm{tot}}$ can be directly used for guiding RSU deployment.

In this example, the total time covered is maximized at the critical distance ($D_{\mathrm{opt}} = D_{\mathrm{c}}$) despite the speed fluctuations. Thus, the optimal deployment strategy within $D \leq D_{\mathrm{c}}$ is putting the two RSUs at the critical distance $D = D_{\mathrm{c}}$. Note that the numerical analysis is valid only for this specific data set, although we have observed similar behavior considering other data sets as well. Still, if prior knowledge is available about how vehicle trajectories typically look like along a certain highway segment, one can find the optimal RSU deployment strategy by evaluating $T^{\mathrm{c}}_{\mathrm{tot}}$ or $T^{\mathrm{p}}_{\mathrm{tot}}$.

Finally, the total time covered $T^{\mathrm{p}}_{\mathrm{tot}}$ for the five-RSU baseline is also indicated by a black line in Fig. 8(c). The maximum amount of available traffic predictions (total time covered $T^{\mathrm{p}}_{\mathrm{tot}}$) for two RSUs is about 75% of the five-RSU baseline, while the instrumentation costs (number of RSUs) are reduced to 40%. Meanwhile, the two-RSU

setup provides the same potential coverage zone duration as the five-RSU baseline; see Fig. 8(a) at $D = D_c = 2000\,\mathrm{m}$. Therefore, the optimal two-RSU deployment strategy at the critical distance is a reasonable alternative to the dense RSU installment baseline when deployment costs are of concern.

6. Conclusion

We investigated the ability of connected roadside infrastructure to provide traffic predictions along the highway based on monitoring the trajectories of connected vehicles (CVs) via roadside units (RSUs). We highlighted that the finite range of vehicle-to-infrastructure (V2I) communication enables the RSUs to record segments of CV trajectories, which allow traffic prediction over certain intervals of time. For the case of a single RSU, we derived both analytically and numerically the time intervals when a certain location can potentially receive predictions about future traffic. We quantified the amount of available predictions via proposed metrics called coverage rate and total time covered. Furthermore, we analyzed how the penetration rate of CVs in traffic and the communication range of the RSU affect the availability of predictions. We showed that even as low as 5% penetration of CVs can enable large amount of predictions (around 90% constant coverage rate) given a several hundred meters of RSU communication range.

Based on the above metrics, we proposed strategies for deciding where to deploy RSUs along a highway segment using prior knowledge about local traffic conditions such that the amount of available traffic prediction is maximized. We determined the optimal distance of two neighboring RSUs. We found that it is beneficial to place the RSUs farther away from each other (around a so-called critical distance) so that their predictions do not overlap. The performance of this deployment strategy was compared to a baseline method involving a dense network of RSUs, and our sparse RSU deployment strategy was justified to be preferable considering the trade-off between available traffic prediction and RSU deployment cost. Although the analysis in this paper was restricted to at most two RSUs for simplicity, the proposed deployment strategy can be applied straightforwardly to design the placement of larger numbers of RSUs. On one hand, one can deploy RSUs sequentially by utilizing the results obtained for the two RSU case. On the other hand, the metrics introduced in this paper can be evaluated for any number of RSUs.

For the sake of numerical case studies, we used a simulated traffic flow where the trajectory of the lead vehicle was taken from experimental data. Our future work will focus on experiments to validate our results. We plan to collect trajectory data from CVs by using RSUs on highways in field experiments, and we plan to analyze the available traffic predictions by utilizing the collected data. We also plan to add other sensors in our experiment, such as cameras, to gather more information about the traffic and facilitate the traffic prediction.

Acknowledgements

This research was partially supported by the University of Michigan's Center of Connected and Automated Transportation through the US DOT grant 69A3551747105.

References

[1] N. Lu, N. Cheng, N. Zhang, X. Shen, J. W. Mark, Connected vehicles: Solutions and challenges, IEEE Internet of Things Journal 1 (4) (2014) 289–299.

[2] C. Wietfeld, C. Ide, Vehicle-to-infrastructure communications, Woodhead Publishing Series in Electronic and Optical Materials, Woodhead Publishing, 2015, pp. 3–28.

[3] J. Chang, An overview of USDOT connected vehicle roadside unit research activities, Tech. rep., Noblis, Inc., U.S. Department of Transportation, Federal Highway Administration Intelligent Transportation Systems (ITS) Joint Program Office, Technical Report FHWA-JPO-17-433 (2017).

[4] Y. Sun, X. Lin, R. Lu, X. Shen, J. Su, Roadside units deployment for efficient short-time certificate updating in VANETs, in: Proceedings of the 2010 IEEE International Conference on Communications, Cape Town, South Africa, 2010, pp. 1–5.

[5] P.-C. Lin, Optimal roadside unit deployment in vehicle-to-infrastructure communications, in: Proceedings of the 12th International Conference on ITS Telecommunications, Taipei, Taiwan, 2012, pp. 796–800.

[6] J. Barrachina, P. Garrido, M. Fogue, F. J. Martinez, J. Cano, C. T. Calafate, P. Manzoni, Road side unit deployment: a density-based approach, IEEE Intelligent Transportation Systems Magazine 5 (3) (2013) 30–39.

[7] J.-H. Jiang, S.-C. Shie, J.-Y. Tsai, Roadside unit deployment based on traffic information in VANETs, in: J.-S. Pan, V. Snasel, E. S. Corchado, A. Abraham, S.-L. Wang (Eds.), Intelligent Data analysis and its Applications, Volume I, Springer, 2014, pp. 355–365.

[8] M. Fogue, J. A. Sanguesa, F. J. Martinez, J. M. Marquez-Barja, Improving roadside unit deployment in vehicular networks by exploiting genetic algorithms, Applied Sciences 8 (1) (2018) 86.

[9] D. L. Moura, R. S. Cabral, T. Sales, A. L. Aquino, An evolutionary algorithm for roadside unit deployment with betweenness centrality preprocessing, Future Generation Computer Systems 88 (2018) 776–784.
[10] H. Yang, Z. Jia, G. Xie, Delay-bounded and cost-limited RSU deployment in urban vehicular ad hoc networks, Sensors 18 (9) (2018) 2764.
[11] S. Ben Chaabene, T. Yeferny, S. Ben Yahia, A roadside unit deployment framework for enhancing transportation services in Maghrebian cities, Concurrency and Computation: Practice and Experience 33 (1) (2019) e5611.
[12] J. Lee, S. Ahn, Adaptive configuration of mobile roadside units for the cost-effective vehicular communication infrastructure, Wireless Communications and Mobile Computing 2019 (2019) 6594084.
[13] Y. Liang, Z. Wu, J. Hu, Road side unit location optimization for optimum link flow determination, Computer-Aided Civil and Infrastructure Engineering 35 (1) (2020) 61–79.
[14] P. S. A. Boukerche, Y. Tao, Artificial intelligence-based vehicular traffic flow prediction methods for supporting intelligent transportation systems, Computer Networks 182 (2020) 107484.
[15] T. Seo, A. M. Bayen, T. Kusakabe, Y. Asakura, Traffic state estimation on highway: A comprehensive survey, Annual Reviews in Control 43 (2017) 128–151.
[16] I. Morărescu, C. Canudas-de-Wit, Highway traffic model-based density estimation, in: Proceedings of the American Control Conference, 2011, pp. 2012–2017.
[17] J. C. Herrera, A. M. Bayen, Incorporation of Lagrangian measurements in freeway traffic state estimation, Transportation Research Part B 44 (4) (2010) 460–481.
[18] X. Feng, X. Ling, H. Zheng, Z. Chen, Y. Xu, Adaptive multi-fernel SVM with spatial–temporal correlation for short-term traffic flow prediction, IEEE Transactions on Intelligent Transportation Systems 20 (6) (2019) 2001–2013.
[19] T. G. Molnár, D. Upadhyay, M. Hopka, M. Van Nieuwstadt, G. Orosz, Delayed Lagrangian continuum models for on-board traffic prediction, Transportation Research Part C 123 (2021) 102991.
[20] D. B. Work, S. Blandin, O.-P. Tossavainen, B. Piccoli, A. M. Bayen, A traffic model for velocity data assimilation, Applied Mathematics Research eXpress 2010 (1) (2010) 1–35.
[21] B. Mehran, M. Kuwahara, F. Naznin, Implementing kinematic wave theory to reconstruct vehicle trajectories from fixed and probe sensor data, in: Proceedings of the 19th International Symposium on Transportation and Traffic Theory, Vol. 17, 2011, pp. 247–268.
[22] S. Wong, L. Jiang, R. Walters, T. G. Molnár, G. Orosz, R. Yu, Traffic forecasting using V2V communication, Proceedings of Machine Learning Research (2021) accepted.
[23] J. C. Herrera, D. B. Work, R. Herring, X. Ban, Q. Jacobson, A. M. Bayen, Evaluation of traffic data obtained via GPS-enabled mobile phones: The Mobile Century field experiment, Transportation Research Part C 18 (4) (2010) 568–583.
[24] Y. Yuan, H. Van Lint, F. Van Wageningen-Kessels, S. Hoogendoorn, Network-wide traffic state estimation using loop detector and floating car data, Journal of Intelligent Transportation Systems 18 (1) (2014) 41–50.
[25] M. L. Delle Monache, T. Liard, B. Piccoli, R. Stern, D. Work, Traffic reconstruction using autonomous vehicles, SIAM Journal on Applied Mathematics 79 (5) (2019) 1748–1767.
[26] H. Yu, Q. Gan, A. M. Bayen, M. Krstic, PDE traffic observer validated on freeway data, IEEE Transactions on Control Systems Technology (2020) published online.
[27] B. S. Kerner, The Physics of Traffic, Springer, 2004.
[28] R. P. Roess, E. L. Prassas, W. R. McShane, Traffic Engineering, 5th Edition, Prentice-Hall, 2019.
[29] D. Ni, Traffic Flow Theory, Butterworth-Heinemann, 2016.
[30] G. Orosz, R. E. Wilson, G. Stépán, Traffic jams: dynamics and control, Philosophical Transactions of the Royal Society A 368 (1928) (2010) 4455–4479.
[31] M. J. Lighthill, G. B. Whitham, On kinematic waves II. A theory of traffic flow on long crowded roads, Proceedings of the Royal Society A 229 (1178) (1955) 317–345.
[32] P. I. Richards, Shock waves on the highway, Operations Research 4 (1) (1956) 42–51.
[33] G. F. Newell, A simplified theory of kinematic waves in highway traffic, part I: General theory, Transportation Research Part B 27 (4) (1993) 281–287.
[34] A. Aw, A. Klar, M. Rascle, T. Materne, Derivation of continuum traffic flow models from microscopic follow-the-leader models, SIAM Journal on Applied Mathematics 63 (1) (2002) 259–278.
[35] J. A. Laval, L. Leclercq, The Hamilton-Jacobi partial differential equation and the three representations of traffic flow, Transportation Research Part B 52 (2013) 17–30.
[36] L. Leclercq, J. Laval, E. Chevallier, The Lagrangian coordinates and what it means for first order traffic flow models, in: Proceedings of the 17th International Symposium on Transportation and Traffic Theory, 2007, pp. 735–753.
[37] G. F. Newell, A simplified car-following theory: a lower order model, Transportation Research Part B 36 (3) (2002) 195–205.
[38] C. F. Daganzo, The cell transmission model: A dynamic representation of highway traffic consistent with the hydrodynamic theory, Transportation Research Part B 28 (4) (1994) 269–287.
[39] P. Berg, A. Mason, A. Woods, Continuum approach to car-following models, Physical Review E 61 (2) (2000) 1056–1066.
[40] A. Aw, M. Rascle, Resurrection of "second order" models of traffic flow, SIAM Journal on Applied Mathematics 60 (3) (2000) 916–938.
[41] H. M. Zhang, A non-equilibrium traffic model devoid of gas-like behavior, Transportation Research Part B 36 (3) (2002) 275–290.
[42] M. Garavello, B. Piccoli, Traffic flow on a road network using the Aw-Rascle model, Communications in Partial Differential Equations 31 (2) (2006) 243–275.
[43] W.-L. Jin, On the equivalence between continuum and car-following models of traffic flow, Transportation Research Part B 93 (A) (2016) 543–559.